

Published in final edited form as:

Nature. 2014 November 27; 515(7528): 587–590. doi:10.1038/nature13722.

Epigenetic reprogramming that prevents transgenerational inheritance of the vernalized state

Pedro Crevillén^{1,†}, Hongchun Yang¹, Xia Cui², Christiaan Greeff^{1,†}, Martin Trick¹, Qi Qiu², Xiaofeng Cao², and Caroline Dean¹

¹Department of Cell & Developmental Biology, John Innes Centre, Norwich Research Park, Norwich NR4 7UH

²State Key Laboratory of Plant Genomics and National Center for Plant Gene Research, Institute of Genetics and Developmental Biology, Chinese Academy of Sciences. Beijing 100101, P.R. China

Abstract

Reprogramming of epigenetic states in gametes and embryos is essential for correct development in plants and mammals¹. In plants, the germ line arises from somatic tissues of the flower necessitating erasure of chromatin modifications accumulated at specific loci during development or in response to external stimuli. If this occurs inefficiently it can lead to epigenetic states being inherited from one generation to the next^{2–4}. However, in most cases accumulated epigenetic modifications are efficiently erased before the next generation. An important example of epigenetic reprogramming in plants is the resetting of expression of the *Arabidopsis thaliana* floral repressor *FLC* locus. *FLC* is epigenetically silenced by prolonged cold in a process called vernalization. However, the locus is reactivated prior to completion of seed development to ensure a vernalization requirement every generation. In contrast to our detailed understanding of the Polycomb-mediated epigenetic silencing induced by vernalization, little is known about the mechanism involved in the re-activation of *FLC*. Here we show that a hypomorphic mutation in the jumonji domain protein ELF6 impaired the reactivation of *FLC* in reproductive tissues, leading to inheritance of a partially vernalized state. ELF6 has H3K27me3 demethylase activity and the mutation reduced this enzymatic activity *in planta*. Consistent with this, H3K27me3 levels at the *FLC* locus stayed higher and *FLC* expression remained lower, than in the wild type in the following generation. Our data reveal an ancient role for H3K27 demethylation in the reprogramming of epigenetic states in plant and mammalian embryos^{5–7}.

Many *Arabidopsis thaliana* accessions overwinter before flowering through FRIGIDA-mediated high-level expression of a floral repressor called FLC^{8,9}. Prolonged cold during

Correspondence and requests for materials should be addressed to C.D. (caroline.dean@jic.ac.uk).

[†]Present addresses: Centro de Biotecnología y Genómica de Plantas, UPM-INIA, 28223 Madrid, Spain (P.C.). Department of Biology, Copenhagen University, DK-2200 Copenhagen, Denmark (C.G.)

Author contributions: P.C. and C.D. designed the research. P.C., H.Y., X. Cui, M.C.G. and Q.Q. performed research. M.T. conducted deep sequencing data analysis. X. Cao contributed with new reagents and analytical tools. P.C., H.Y. and C.D. analysed data and wrote the paper. All authors discussed the results and commented on the manuscript.

The authors declare no competing financial interests.

Reprints and permissions information is available at www.nature.com/reprints.

the weeks of winter antagonizes this activation and progressively epigenetically silences *FLC*. This enables other floral promotion signals such as day length to induce flowering in spring. The epigenetic silencing of *FLC* involves Polycomb-mediated chromatin regulation¹⁰⁻¹² and is maintained until embryogenesis, when *FLC* expression is reset to ensure a vernalization requirement every generation^{13,14}. Resetting of *FLC* expression occurs in the early globular embryo^{13,14}; then, *FLC* expression increases throughout embryo development until it reaches maximum levels when the seed is completely formed¹⁴. However, the molecular mechanisms underlying *FLC* resetting are unknown, and the testing of several factors known to be required for the up-regulation of *FLC* in vegetative tissues showed they were dispensable for *FLC* expression in the embryo¹⁴. One exception is the yeast SWR1 homolog PIE1¹⁴, although it is not clear if this a resetting-specific defect because *pie1* mutations strongly reduce *FLC* expression across the plant independently of vernalization status.

In order to dissect this resetting mechanism we isolated mutants defective in the reactivation of *FLC* after vernalization (Extended Data Fig. 1a). The parental line was an Arabidopsis *Landsberg erecta* (*Ler*) plant carrying an *FLC::luciferase* (*FLC::LUC*) translational fusion and an active *FRIGIDA* (*FRI*) transgene¹⁵. We searched for plants where *FLC* expression pre-vernalization was silenced by vernalization but unlike wild type was not fully restored in the following generation (Fig. 1a), leading to inheritance of the vernalized state. The frequency of these mutations was low (only 2 mutants identified from progeny of 6,000 mutagenized parent lines), contrasting with the more common class of mutations, which were early flowering before vernalization due to reduced *FLC* expression (Extended Data Fig. 1b). The first resetting mutant isolated was found to be recessive (Extended Data Fig. 2a) and was slightly earlier flowering without vernalization than the wild type (Fig. 1b). In the generation following vernalization the mutant was even earlier flowering and had significantly reduced *FLC* expression (Fig. 1c,d), albeit ~four fold higher than fully vernalized seedlings (Fig. 1d). The resetting mutant therefore causes transgenerational inheritance of a partially vernalized state. The early flowering phenotype was stable for at least 3 generations following vernalization (Extended Data Fig. 2b) but was not enhanced by a second vernalization treatment in the later generations. There were no other strong developmental phenotypes.

The mutant phenotype was strongly affected by segregation of modifiers in a traditional *Ler* X Columbia (*Col*) cross, normally used for genetic mapping, and the mutation could only be narrowed down to a ~500 kb region on chromosome 5. We therefore sequenced the whole genome of the mutant plant and analysed linkage of candidate SNPs in an F2 population generated from a cross between the mutant and the isogenic progenitor line. This strategy identified a single nucleotide polymorphism in *ELF6* (*At5g04240*) that co-segregated with the resetting phenotype (Extended Data Fig. 3). To confirm that the resetting phenotype was indeed caused by the *elf6-5* mutant allele, we complemented the mutation using *ELF6* gene under its own regulatory sequences. Vernalized T2 transgenic lines carrying the wild-type *ELF6* transgene showed wild-type *FLC* expression levels in the siliques (Fig. 2a,b). Thus, we concluded that the single nucleotide mutation in *ELF6* caused the mutant phenotype.

ELF6 is a jumonji C (JmJC) domain protein closely related to the histone H3 lysine 27 (H3K27me3) demethylase REF6¹⁶ and it is expressed at low levels in seedlings but at high levels in flowers and embryos (Fig 2c-f). The *elf6-5* mutation changes an alanine to valine (amino acid 424) at the carboxy terminal end of the JmJC domain (Fig. 2g). This amino acid is conserved in REF6 and the human H3K27me3 demethylases UTX (also known as KDM6A) and JMD3 (also known as KDM6B) (Fig. 2g). This high degree of conservation suggests that this residue may be crucial to the function of the protein. A null *ELF6* T-DNA insertion allele is early flowering due to increased expression of *FT*¹⁷, an integrator gene that promotes floral transition. In addition, we found reduced *FLC* expression in an *elf6-3* KO allele compared to wild-type *Col* (Extended Data Fig. 4a), confirming that ELF6 regulates *FLC* expression. The early flowering phenotype and low *FLC* expression in *elf6-3* precluded seeing the resetting phenotype (Extended Data Fig. 4b). Although different genetic backgrounds of the two alleles may complicate interpretation these data suggest that the *elf6-5* alanine to valine substitution confers a hypomorphic phenotype affecting an activity particularly important for resetting *FLC* expression during reproductive development.

Consistent with a role in regulating *FLC* resetting, *elf6-5* had a much larger effect on *FLC* expression in flowers and siliques as compared to seedlings (Figs. 3a,b). To define more precisely when the *elf6-5* mutant disrupted *FLC* expression we measured *FLC* mRNA levels at different stages of silique development¹⁸, a proxy for *FLC* expression in the embryo^{13,14}. Low *FLC* mRNA levels could be detected in young siliques from the vernalized parental line (SQ16 and SQ17a) (Fig. 3c), which increased as the silique matured (SQ17b1 and SQ17b2) to a maximum as the silique started to desiccate and the embryo fully developed (SQ18). In the vernalized resetting mutant, *FLC* mRNA was detected in young developing siliques but it was not up regulated to wild-type levels at the later stages (Fig. 3c). Comparison of sibs differing only by a *FLC::GUS* reporter¹⁹ showed *FLC::GUS* expression was lower in early globular embryo of *elf6-5* compared to wild type (Fig. 3d). This suggests ELF6 increases *FLC* expression as the embryo develops. There may be no clear mechanistic separation between reprogramming of the epigenetic state and setting of expression level.

The *FLC* locus has a complex transcriptional circuitry including a set of antisense transcripts called *COOLAIR* that are induced during vernalization but are also expressed in the warm²⁰. We wondered if the resetting mutant also affected *COOLAIR* expression. Surprisingly, no change between mutant and wild type was found and total *COOLAIR* transcripts were up regulated normally in the mutant in developing siliques (Fig. 3e). Therefore, in contrast to mutations where both *FLC* sense and total *COOLAIR* expression levels are changed coordinately, for example *fri*, the *elf6-5* mutation uncouples *FLC* sense and antisense regulation.

Many other loci are epigenetically modified during Arabidopsis gamete formation and embryo development^{21,22}. We tested if *elf6-5* would influence transposon expression by analyzing specific siRNA produced during seed development²²; including an siRNA homologous to the flanking 3' region of the *FLC* locus that accumulates preferentially in siliques²³. Using sensitive northern blot analyses we could not detect any difference in the amount of these siRNAs in *elf6-5* when compared to parental line using vernalized siliques

(Extended Data Fig. 5). We then asked whether *elf6-5* influenced expression of other *FLC*-family members²⁴. *MAF2*, *MAF3*, *MAF4* and *MAF5* expression were down regulated in *elf6-5* seedlings and expressed below detection levels in siliques (Fig. 3f); whereas *FLM/MAF1* expression was unchanged in seedlings but strongly down regulated in *elf6-5* siliques (Fig. 3f,g). Vernalization response in winter-annual Arabidopsis accessions (containing an active *FRI* allele) depends predominantly on *FLC* activity²⁴, but in the rapid-cycling Col (*fri*) genotype all *MAF* genes appear to be direct targets of the Polycomb machinery^{24,25} indicating that the ELF6-regulatory mechanism elaborated for *FLC* may have more general functions in the Arabidopsis genome.

Since ELF6 is closely related to the H3K27me3 demethylase REF6 we tested both wild-type and mutant ELF6 enzymatic activity using an *in vivo* histone demethylation assay¹⁶. We found that transient expression of Arabidopsis ELF6 resulted in reduced H3K27me2 and H3K27me3 levels in tobacco leaves (Fig. 4a); no changes were found in H3K27me1, H3K4me3, H3K9me2 and H3K36me3 (Fig. 4a and Extended Data Fig. 6). These data show that Arabidopsis ELF6 has histone demethylase activity specific for H3K27me2 and H3K27me3. The *elf6-5* mutation is an alanine to valine substitution at the carboxy terminal end of the JmJC domain. The mutation of this highly conserved residue (Fig. 2g) thus reduced the H3K27 demethylase activity in our assay (Fig. 4b). To test if this reduced activity influenced H3K27me3 levels *in vivo* at *FLC* locus, we performed chromatin immunoprecipitation experiments (ChIP). In wild-type *Ler-FRI* plants, H3K27me3 levels increase about 2-4 fold in vernalized seedlings, but were reduced to almost non-vernalized levels in vernalized siliques (Extended Data Fig. 7). When the resetting mutant was analysed, we found that H3K27me3 levels were higher at *FLC* in *elf6-5* compared to the parental line on vernalized young siliques (Fig. 4d). ChIP analysis on seedlings the generation following vernalization also showed increased levels of H3K27me3 over different *FLC* regions in *elf6-5* (Fig. 4e). These experiments were performed using whole seedlings or siliques, therefore data should be interpreted cautiously because they comprise a mixture of tissues. The vernalization-independent increase in H3K27me3 in *elf6-5* and the phenotype of the *elf6* loss-of-function mutant makes it likely that ELF6 has broader functions than just resetting H3K27 methylation after vernalization. Nevertheless, all these data are consistent with reduced *FLC* expression during embryo development in *elf6-5* involving perturbed H3K27me3 dynamics that affects *FLC* resetting and results in inheritance of a partial vernalized state.

This effective impairment in reducing H3K27me3 levels at *FLC* leads to transgenerational inheritance of a partially vernalized state (Fig. 1a-d). The consequences of this in nature would be to misalign the developmental program of the plant with respect to the environmental conditions. The sensitivity of *FLC* resetting to the reduced function *elf6-5* allele may indicate the requirement for H3K27me3 demethylase activity is highest at this post-vernalization stage of development, potentially explaining the differences in phenotype between *elf6-5* and the null allele *elf6-3*. Functional redundancy between the three close homologues REF6, ELF6 and *AtJMJ13*(AT5G46910) may also vary through development¹⁶. It will be interesting to see if histone variants known to change in expression during embryogenesis are also involved in *FLC* resetting²⁶. The large proportion of the chromatin

in most eukaryotic genomes decorated with H3K27me3 probably accounts for why its erasure is a tightly controlled event during development and germ cell formation²⁷. Further characterization of the *FLC* resetting process should provide greater insight into the molecular mechanism underlying genome reprogramming in eukaryotic organisms.

Methods

Plant material and growth conditions

All genotypes except *elf6-3*¹⁷ were in a *Landsberg erecta* (*Ler*) background; an active *FRIGIDA JU223* allele and a genomic *FLC::LUC* construct were introduced by transformation to generate a vernalization responsive line where *in vivo FLC* expression could be monitored by luciferase imaging¹⁵. Genetic analyses and flowering time experiments were performed with plant sown on soil and grown in controlled environment chambers in long day conditions (16 h light at 22 °C, 8 h darkness at 20 °C). To vernalize, seeds were pre-grown for 7 days at long day warm growing conditions before being transferred to cold (8 h light and 16 h darkness at 5 °C) for 6 weeks, and then returned to warm conditions.

Flowering time

was scored as the total leaf number, including rosette and cauline leaves, before the first flower opened. Statistical evaluations were performed by Student's *t*-test.

Reporter gene analysis

Parental *Ler-FRI*, *FLC::LUC* line was described previously¹⁵ and luciferase imaging was detected using a Nightowl imaging system (Berthold). Siliques valves were opened longitudinally to detect *FLC::LUC* signal from developing embryos. A complementing *pELF6::ELF6::GUS::ELF6-3'UTR* construction in *elf6-1* mutant background was used to monitor ELF6 expression. *FLC::GUS*¹⁹ was introgressed into the resetting mutant and β-glucuronidase activity was detected in Arabidopsis embryos. Siliques were longitudinally cut, fixed for 2 h at 20°C in 90% acetone and washed three times with 50 mM phosphate buffer (pH 7.0) before incubation at 37°C in reaction buffer for 24h (0.19 mM 5-bromo,4-chloro,3-indolyl-D-glucuronide, 10 mM EDTA, 0.1% Triton X-100, 0.1 mM KFeCN, 50 mM phosphate buffer pH 7.2). Embryos were observed after clearing in Hoyer's medium using a microscope under bright-field Nomarski optics.

RNA expression analysis

For seedlings RNA analysis seeds were sown on GM media plates, stratified for 2 days and grown in long day conditions for 11 days. RNA extraction from seedlings, DNase I treatment, cDNA synthesis, real-time quantitative PCR analyses and primers for *FLC*, total *COOLAIR* antisense and *UBC* control gene were described in Crevillén *et al* (2013)²⁸. Primers for MAF genes detection were described before^{29,30}. For the study of *FLC* expression in reproductive tissues, each biological replicate was obtained extracting RNA³¹ from the main inflorescence or 3-5 siliques from 5 different plants. Expression data represents the average a several biological replicates as stated in the figure legends. Statistical evaluations were performed by Student's *t*-test.

Illumina sequencing

To identify the resetting mutation we performed genomic DNA deep sequencing from both the parental, *Ler*-derived plant and the resetting mutant line (EBI accession number PRJEB6498). Total genomic DNA was isolated from 2 g of inflorescences following a standard procedure. Briefly, inflorescences were grinded in liquid nitrogen, samples were homogenized in Extraction Buffer (50mM Tris pH 8; 200 mM NaCl; 2 mM EDTA; 0.5% SDS; 100 mg/ml Proteinase K), and incubated at 37 °C for 30 min. Proteins were removed by phenol/chloroform extraction, and DNA was precipitated using 2.5 volumes ethanol and in presence of 3M sodium acetate (pH 5).

Illumina libraries were prepared using genomic DNA. The Illumina GAIIX sequencing platform was used to generate 76 base, paired-end reads for each sample. The alignment program Maq³² v0.7.1 was used, first of all, to map reads from the parental line against the Col-0 (TAIR6) reference sequence. For this parental line, 10,867,014 reads from a total of 14,455,072 were mapped (with 10,265,540 of these in pairs). 40,573 high confidence SNPs identified with the companion maq.pl Perl script were then used, in combination with a list of *Ler* SNPs (<http://signal.salk.edu/atg1001/data/>), to edit the original Col-0 reference sequence for use in the subsequent alignment with reads obtained from the mutant line. 58,556,730 reads from a total of 65,673,308 were aligned against this modified reference sequence, with 55,308,855 of these in pairs, resulting in average 34X coverage. A local instance of the GBrowse genome browser³³ was created and loaded with the modified pseudochromosome sequences and TAIR6 coordinate-based gene model annotations. The mutant SNPs, relative to the Col-0/*Ler*/parental-adapted reference sequence, were then loaded into the GBrowse MySQL database and made available for visual inspection as an added feature track. By programmatically interrogating the database with a Perl script using Bio::DB::GFF methods, a genome-wide total of 417 EMS candidates (G/A -> C/T in annotated coding sequence and inferred to induce either non-synonymous codon or donor/acceptor splice site mutations) were then identified for further study.

Genetic complementation

A genomic fragment including the *ELF6* locus was amplified from wild-type *Ler* genomic DNA using the primers 5'-ATGCCAATCCCAGAAAGTTG-3' and 5'-AGGAGTCGTTGTCACGCTTA-3', and cloned into pGEM-T vector (Promega). A 7.35 Kb *SacI* – *KpnI* fragment including full genomic *ELF6* and regulatory regions (1.1kb from promoter and 860 bp downstream of stop codon) was cloned into pCAMBIA1300 binary vector (www.cambia.org). Resetting mutant plants were transformed by floral dipping and hygromycin resistant T1 plants isolated. For complementation analyses parental (*Ler-FRI*, *FLC::LUC*), mutant and independent T2 lines were vernalized and *FLC* luciferase activity measured in siliques: 8 out of 10 transgenic T2 lines analysed complemented the resetting phenotype. As a control experiment all T2 lines were also sown without antibiotic selection and plants not carrying the transgene were analysed: all lines without the transgenic *ELF6* construct failed to complement the resetting phenotype.

Sequence alignment

The amino acid sequence alignment of the JmJC domain of Arabidopsis ELF6 (Q6BDA0), Arabidopsis REF6 (Q9STM3), human JMJD3 (AAH09994) and human UTX (AAT86073) proteins was performed using the web-based software *Multalin* tool³⁴ (<http://multalin.toulouse.inra.fr/multalin/>).

Small RNA analysis

Total RNA extraction and northern blot analysis were performed as described before²³ using seeds specific probes²².

In vivo histone demethylation assay

Wild-type ELF6 or mutant *elf6-5* full genomic coding sequences were cloned into pEG104 vector³⁵. The demethylation assay was carried out as previously described¹⁶. Briefly, *N. benthamiana* leaves were infiltrated with *A. tumefaciens* EHA105 strains carrying a functional wild-type 35S::YFP::ELF6 or mutant 35S::YFP::ELF6^{A424V}. Transfected nuclei were isolated after 48 h. Immunolabeling of fixated nuclei was performed using histone methylation-specific antibodies: H3K4me3 Millipore 07-473, 1:100; H3K9me2 Millipore 07-441, 1:200; H3K27me3 Millipore 07-449, 1:100; H3K27me2 Millipore 07-452, 1:200; H3K27me1 Millipore 07-448, 1:200; H3K36me3 Abcam 9050, 1:100. The modified histones were revealed by Alexa Fluor 555-conjugated goat anti-rabbit (Invitrogen, 1:200). Transfected cells were revealed by monitoring the YFP signal. After staining, the slides were mounted in VECTASHIELD mounting medium with DAPI (Vector Laboratory) and then photographed with an OLYMPUS BX51 fluorescence microscope. Histone methylation levels were quantified by comparing staining density of a number of transfected 35S::YFP::ELF6 nuclei versus non-transfected nuclei in the same field. Image density was determined using ImageJ software. A negative result in our assay usually corresponds to 80% or less than total wild-type histone demethylase activity.

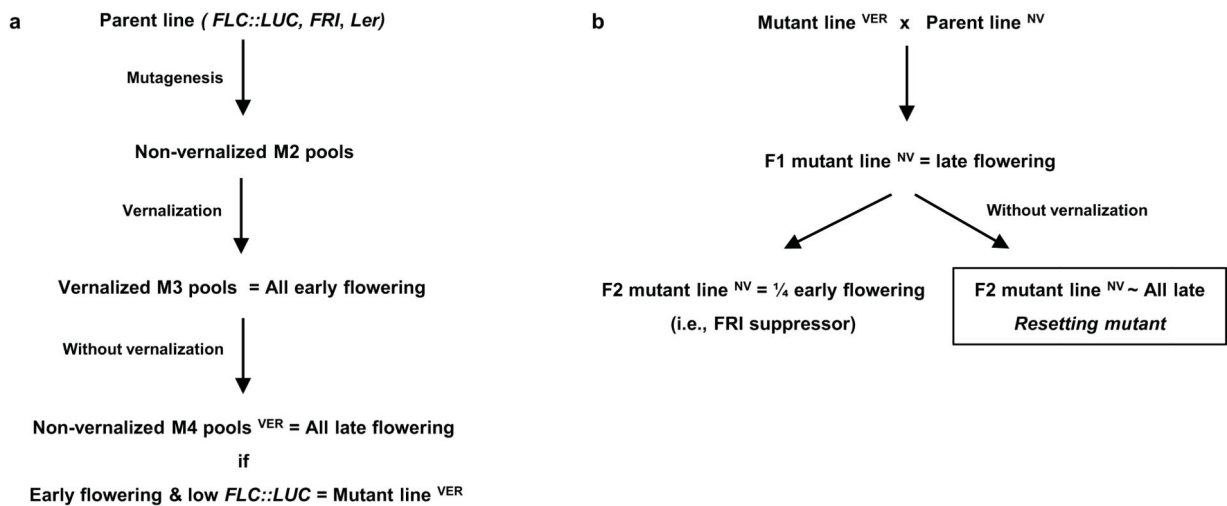
Chromatin Immunoprecipitation experiments

(ChIP) were performed using 11 days old seedlings using the protocol described before¹². For siliques minor modifications were performed. About 0.5 g of tissue was grinded in liquid nitrogen, and then the powder was incubated for 10 min at room temperature in extraction buffer + 1% formaldehyde to fix the tissue. We used anti-trimethyl-histone H3 lysine 27 (Millipore 07-449) and anti-H3 core antibody (Abcam 1791). All ChIP experiments were quantified by Q-PCR and analysed with the primers described before³⁶. ChIP data is represented as the ratio H3K27me3/totalH3 normalized to non-vernalized wild-type levels. ChIP seedling data was also normalized to *STM* H3K27me3 levels³⁶.

Statistical analysis

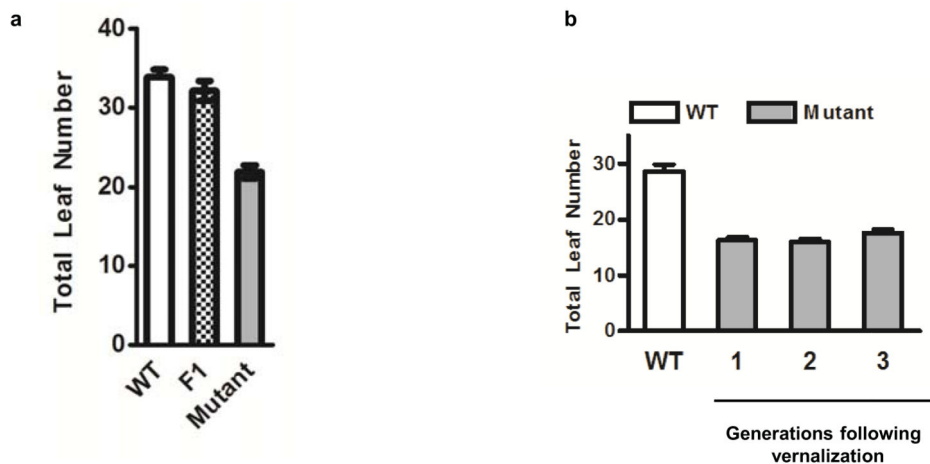
Statistical evaluations by Student's *t*-test and graphical representation of the data were performed using the Prism software package (GraphPad). Means and s.e.m. are derived from independent biological samples.

Extended Data



Extended Data Figure 1. Screening for mutants impaired in the epigenetic reprogramming of *FLC*

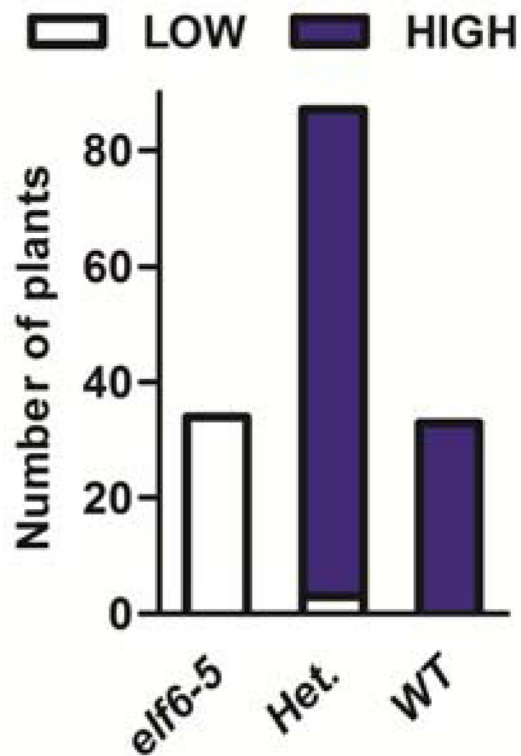
a, We started with a population of EMS-mutagenized *Arabidopsis Landsberg erecta* (*Ler*) plants carrying an *FLC::luciferase* (*FLC::LUC*) translational fusion and an active *FRIGIDA* transgene. The mutants we screened for were early flowering (from low *FLC* expression) in the generation following vernalization, but which did not flower early (and whose *FLC* expression was near normal) without vernalization. **b**, To discriminate early flowering from resetting mutants early flowering M2 plants were backcrossed to the parental line and the F2 phenotype evaluated without vernalization. Those showing no early flowering segregants were considered to be resetting mutants. In the figure, we use superscript characters to note if the plant was vernalized in the previous generation.



Extended Data Figure 2. Characterization of the first *resetting* mutant

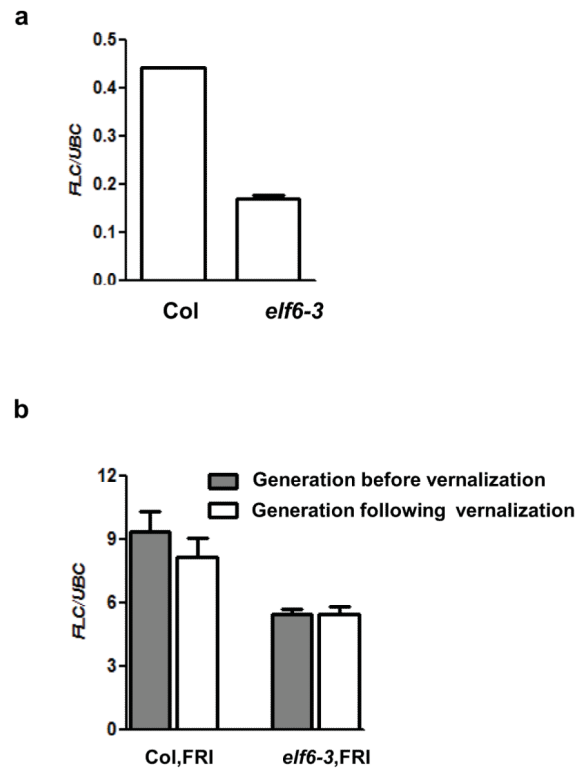
a, The first *resetting* mutation was found to be recessive. F1 plants were generated from a cross between the mutant the generation following vernalization and the parental wild-type line. Flowering time was assayed as total leaf number under non-vernalized long day

conditions. Means + s.e.m., n = 8. **b**, The earlier flowering time of the mutant the generation following vernalization was stable at least three generations without vernalization. Means + s.e.m., n = 10.

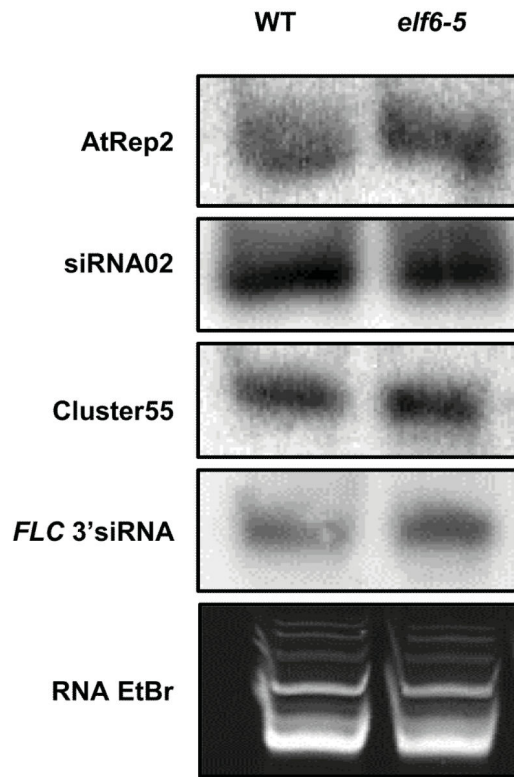


Extended Data Figure 3. The *elf6-5* SNP is linked to resetting of *FLC* expression

Histogram showing the relationship between *FLC::LUC* levels in reproductive organs of vernalized plants and the *elf6-5* SNP (n=154).

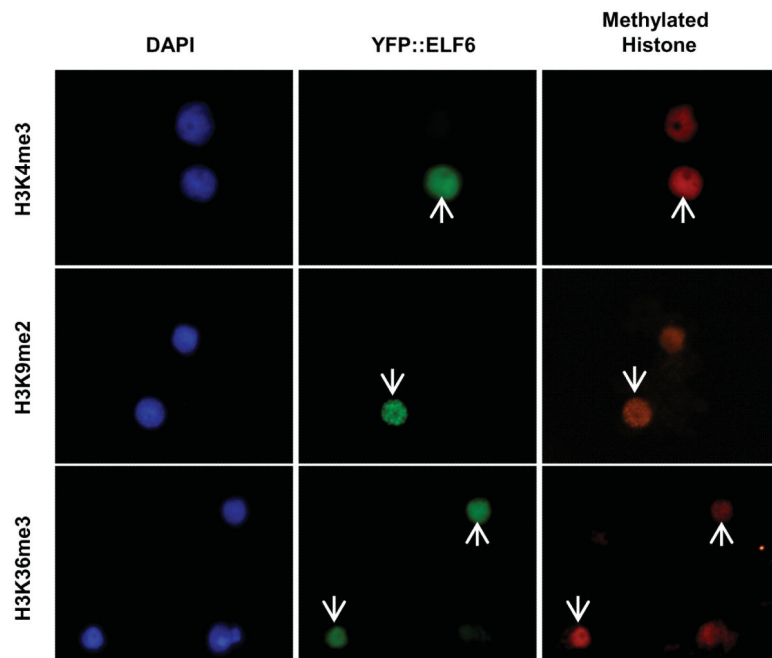


Extended Data Figure 4. *FLC* expression levels in the null *elf6-3* T-DNA insertion allele
a, *elf6-3* shows reduced *FLC* expression compared to *Col* wild-type. **b**, the null *elf6-3* allele suppresses the high *FLC* expression induced by FRI before vernalization. This pre-vernalization phenotype of the null allele precludes observing the role of *ELF6* during *FLC* resetting after vernalization. All graphs show 10 day-old non-vernalized seedlings. Means + s.e.m., n = 3.



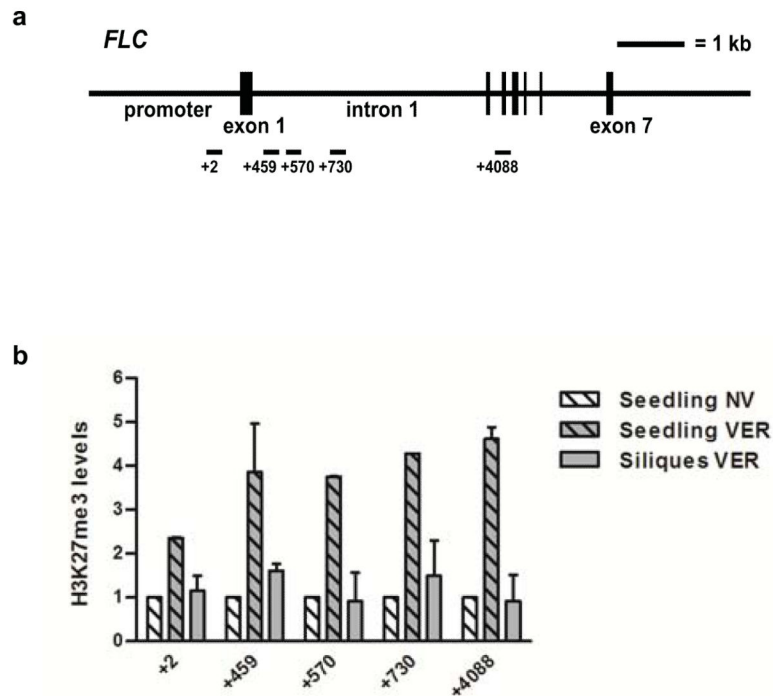
Extended Data Figure 5. siRNA production in *elf6-5*

The production of specific siRNA associated with the epigenetic reactivation of transposable elements is not affected in *elf6-5*. Total RNA was extracted from vernalized mature siliques and detection of siRNAs was performed as described in the Methods.



Extended Data Figure 6. ELF6 has no H3K4/K9/K36me demethylase activity in a *N. benthamiana* transient assay

Overexpression of a YFP-ELF6 fusion protein, using wild-type ELF6 sequence has no effect on H3K4me3/K9me2/K36me3 methylation. Histone methylation was visualized by immunostaining with rabbit polyclonal modification-specific antibodies followed by Alexa fluor 555-conjugated goat anti-rabbit (red; right panels). Transfected nuclei were visualized by the YFP signal (green; middle panels). Nuclei were stained with DAPI (blue; left panels). Arrows indicate transfected nuclei.



Extended Data Figure 7. H3K27me3 accumulation at the *FLC* locus

a, Schematic representation of the *FLC* locus and regions analysed in the chromatin immunoprecipitation. **b**, H3K27me3 levels at *FLC* in *Ler-FRI* seedlings grown without vernalization (Seedling NV), 7 days after vernalization (Seedling VER) and siliques from vernalized seedlings (Siliques VER). Means + s.d., n = 2.

Acknowledgments

We thank Dean lab members and A. Surani for useful discussions. The Dean lab is supported by the UK Biotechnology and Biological Sciences Research Council grants BB/G009562/1 and BB/C517633/1, and a European Research Council Advanced Investigator grant 233039 ENVGENE. The Cao lab is supported by National Basic Research Program of China grants 2013CB967300 and 2011CB915400, and the National Natural Science Foundation of China grant 31271363. C.D. holds stock in Mendel Biotechnology.

References

1. Feng S, Jacobsen SE, Reik W. Epigenetic reprogramming in plant and animal development. *Science*. 2010; 330:622–7. [PubMed: 21030646]
2. Paszkowski J, Grossniklaus U. Selected aspects of transgenerational epigenetic inheritance and resetting in plants. *Curr. Opin. Plant Biol.* 2011; 14:195–203. [PubMed: 21333585]

3. Becker C, et al. Spontaneous epigenetic variation in the *Arabidopsis thaliana* methylome. *Nature*. 2011; 480:245–9. [PubMed: 22057020]
4. Schmitz RJ, et al. Transgenerational epigenetic instability is a source of novel methylation variants. *Science*. 2011; 334:369–73. [PubMed: 21921155]
5. Mansour AA, et al. The H3K27 demethylase Utx regulates somatic and germ cell epigenetic reprogramming. *Nature*. 2012; 488:409–13. [PubMed: 22801502]
6. Canovas S, Cibelli JB, Ross PJ. Jumonji domain-containing protein 3 regulates histone 3 lysine 27 methylation during bovine preimplantation development. *Proc. Natl. Acad. Sci. U.S.A.* 2012; 109:2400–5. [PubMed: 22308433]
7. Zhao W, et al. Jmj3 Inhibits Reprogramming by Upregulating Expression of INK4a/Arf and Targeting PHF20 for Ubiquitination. *Cell*. 2013; 152:1037–1050. [PubMed: 23452852]
8. Johanson U. Molecular Analysis of FRIGIDA, a Major Determinant of Natural Variation in *Arabidopsis* Flowering Time. *Science*. 2000; 290:344–347. [PubMed: 11030654]
9. Sheldon CC, et al. The FLF MADS box gene: a repressor of flowering in *Arabidopsis* regulated by vernalization and methylation. *Plant Cell*. 1999; 11:445–58. [PubMed: 10072403]
10. Gendall AR, Levy YY, Wilson A, Dean C. The VERNALIZATION 2 gene mediates the epigenetic regulation of vernalization in *Arabidopsis*. *Cell*. 2001; 107:525–35. [PubMed: 11719192]
11. Song J, Angel A, Howard M, Dean C. Vernalization - a cold-induced epigenetic switch. *J. Cell Sci*. 2012; 125:3723–31. [PubMed: 22935652]
12. De Lucia F, Crevillén P, Jones AME, Greb T, Dean C. A PHD-polycomb repressive complex 2 triggers the epigenetic silencing of FLC during vernalization. *Proc. Natl. Acad. Sci. U.S.A.* 2008; 105:16831–6. [PubMed: 18854416]
13. Sheldon CC, et al. Resetting of FLOWERING LOCUS C expression after epigenetic repression by vernalization. *Proc. Natl. Acad. Sci. U.S.A.* 2008; 105:2214–9. [PubMed: 18250331]
14. Choi J, et al. Resetting and regulation of Flowering Locus C expression during *Arabidopsis* reproductive development. *Plant J*. 2009; 57:918–31. [PubMed: 19121105]
15. Mylne J, Greb T, Lister C, Dean C. Epigenetic regulation in the control of flowering. *Cold Spring Harb. Symp. Quant. Biol.* 2004; 69:457–64. [PubMed: 16117681]
16. Lu F, Cui X, Zhang S, Jenuwein T, Cao X. *Arabidopsis* REF6 is a histone H3 lysine 27 demethylase. *Nat. Genet.* 2011; 43:715–9. [PubMed: 21642989]
17. Noh B, et al. Divergent roles of a pair of homologous jumonji/zinc-finger-class transcription factor proteins in the regulation of *Arabidopsis* flowering time. *Plant Cell*. 2004; 16:2601–13. [PubMed: 15377760]
18. Roeder AHK, Yanofsky MF. Fruit development in *Arabidopsis*. *Arabidopsis Book*. 2006; 4:e0075. [PubMed: 22303227]
19. Bastow R, et al. Vernalization requires epigenetic silencing of FLC by histone methylation. *Nature*. 2004; 427:164–7. [PubMed: 14712277]
20. Ietswaart R, Wu Z, Dean C. Flowering time control: another window to the connection between antisense RNA and chromatin. *Trends Genet.* 2012; 28:445–53. [PubMed: 22785023]
21. Slotkin RK, et al. Epigenetic reprogramming and small RNA silencing of transposable elements in pollen. *Cell*. 2009; 136:461–72. [PubMed: 19203581]
22. Mosher, R. a, et al. Uniparental expression of PolIV-dependent siRNAs in developing endosperm of *Arabidopsis*. *Nature*. 2009; 460:283–286. [PubMed: 19494814]
23. Swiezewski S, et al. Small RNA-mediated chromatin silencing directed to the 30 region of the *Arabidopsis* gene encoding the developmental regulator, FLC. *Proc. Natl. Acad. Sci. U.S.A.* 2007; 104:3633–8. [PubMed: 17360694]
24. Alexandre CM, Hennig L. FLC or not FLC: the other side of vernalization. *J. Exp. Bot.* 2008; 59:1127–35. [PubMed: 18390846]
25. Kim D-H, Sung S. Coordination of the vernalization response through a VIN3 and FLC gene family regulatory network in *Arabidopsis*. *Plant Cell*. 2013; 25:454–69. [PubMed: 23417034]
26. Ingouff M, et al. Zygotic resetting of the HISTONE 3 variant repertoire participates in epigenetic reprogramming in *Arabidopsis*. *Curr. Biol.* 2010; 20:2137–43. [PubMed: 21093266]

27. Surani MA, Hayashi K, Hajkova P. Genetic and epigenetic regulators of pluripotency. *Cell*. 2007; 128:747–62. [PubMed: 17320511]
28. Crevillén P, Sonmez C, Wu Z, Dean C. A gene loop containing the floral repressor FLC is disrupted in the early phase of vernalization. *EMBO J*. 2013; 32:140–8. [PubMed: 23222483]
29. Gu X, Jiang D, Wang Y, Bachmair A, He Y. Repression of the floral transition via histone H2B monoubiquitination. *Plant J*. 2009; 57:522–33. [PubMed: 18980658]
30. Jiang D, Gu X, He Y. Establishment of the winter-annual growth habit via FRIGIDA-mediated histone methylation at FLOWERING LOCUS C in Arabidopsis. *Plant Cell*. 2009; 21:1733–1746. [PubMed: 19567704]
31. Oñate-Sánchez L, Vicente-Carbajosa J. DNA-free RNA isolation protocols for Arabidopsis thaliana, including seeds and siliques. *BMC Res Notes*. 2008; 1:93. [PubMed: 18937828]
32. Li H, Ruan J, Durbin R. Mapping short DNA sequencing reads and calling variants using mapping quality scores. *Genome Res*. 2008; 18:1851–8. [PubMed: 18714091]
33. Stein LD, et al. The generic genome browser: a building block for a model organism system database. *Genome Res*. 2002; 12:1599–610. [PubMed: 12368253]
34. Corpet F. Multiple sequence alignment with hierarchical clustering. *Nucleic Acids Res*. 1988; 16:10881–10890. [PubMed: 2849754]
35. Earley KW, et al. Gateway-compatible vectors for plant functional genomics and proteomics. *Plant J*. 2006; 45:616–29. [PubMed: 16441352]
36. Angel A, Song J, Dean C, Howard M. A Polycomb-based switch underlying quantitative epigenetic memory. *Nature*. 2011; 476:105–8. [PubMed: 21785438]

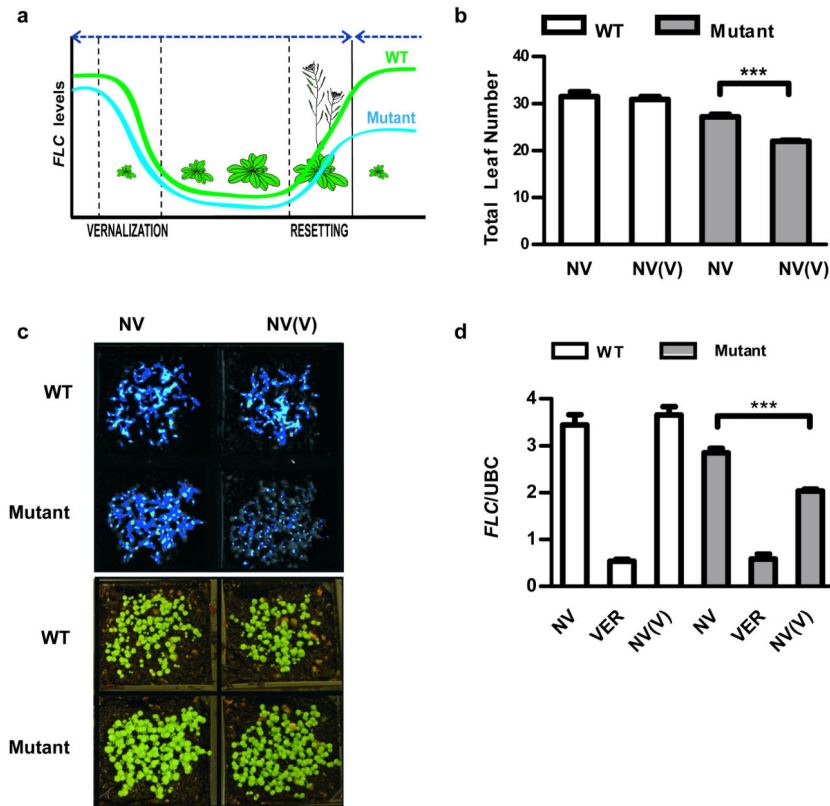


Figure 1. Isolation and characterization of the resetting mutant

a, Logic of the genetic screen. Parental wild-type is *Ler-FRI FLC::luciferase*. **b-d**, The resetting mutant is early flowering (**b**) with fewer total leaves and maintains low *FLC* expression shown by *FLC* luciferase imaging of 8 day-old seedlings (**c**) or Q-RT-PCR analysis normalised to UBC (**d**). NV is non-vernalized, VER is vernalized, NV(V) is non-vernalized following vernalization in the previous generation. Means + s.e.m., $n = 20$ (**b**) and $n = 3$ (**d**), *** $P < 0.001$.

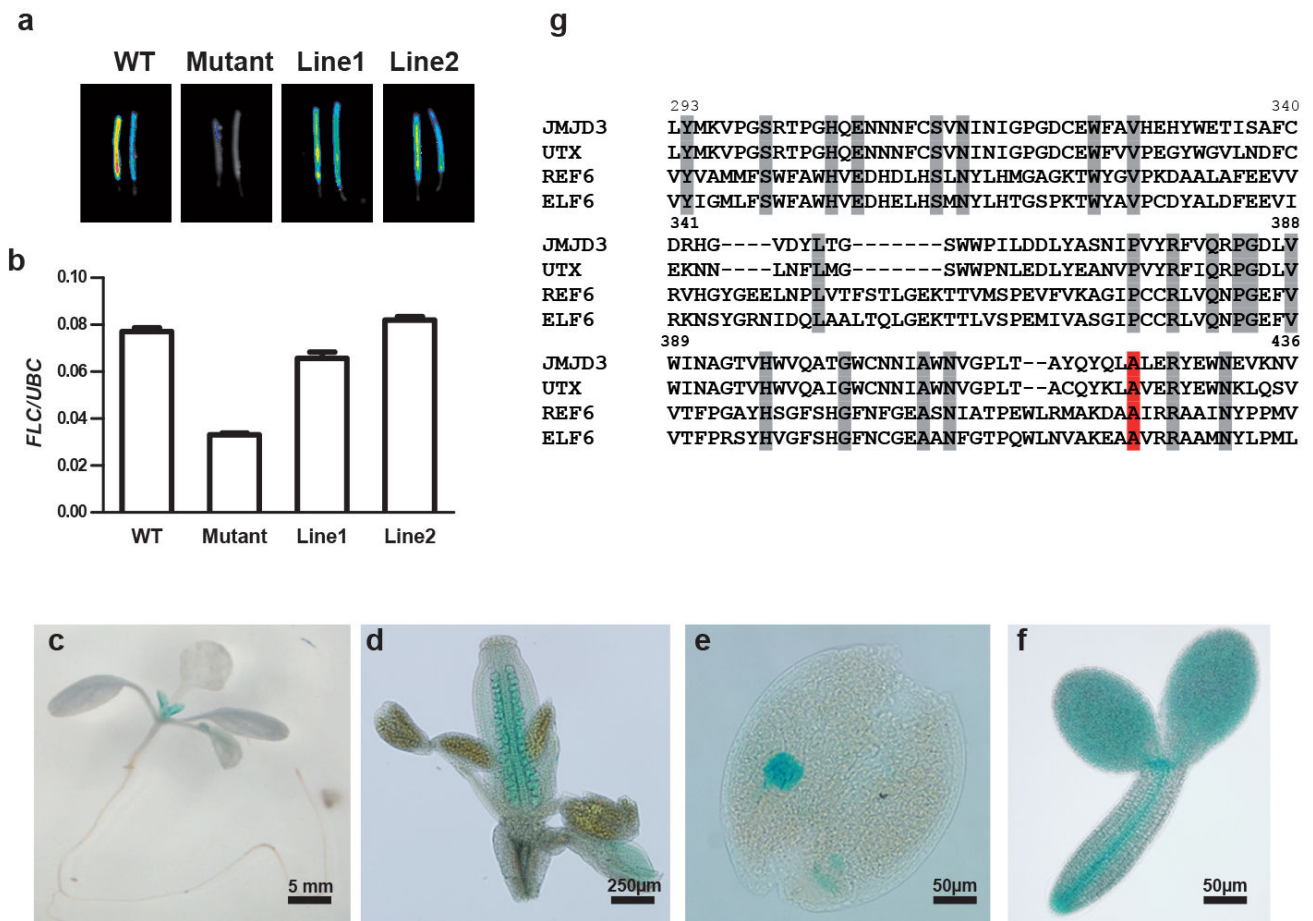


Figure 2. Mapping of the resetting mutant

a, b *ELF6* genomic construct complements the resetting mutant. *FLC* luciferase imaging (**a**) and *FLC* Q-RT-PCR data (**b**) of mature siliques from vernalized WT, *elf6-5* and representative T2 *elf6-5* [*pELF6::ELF6*] lines. **c-f**, *ELF6::GUS* expression profile in 7 day-old seedling (**c**), ovules (**d**), globular embryo (**e**) and mature embryo (**f**). **g**, The *ELF6* residue mutated in *elf6-5* is conserved (red A). Sequence alignment of the JmJC domain of Arabidopsis *ELF6* and *REF6*, and human *JMJD3* and *UTX* proteins. Highly conserved residues are shadowed in grey. Numbering refers to *ELF6* amino acid position.

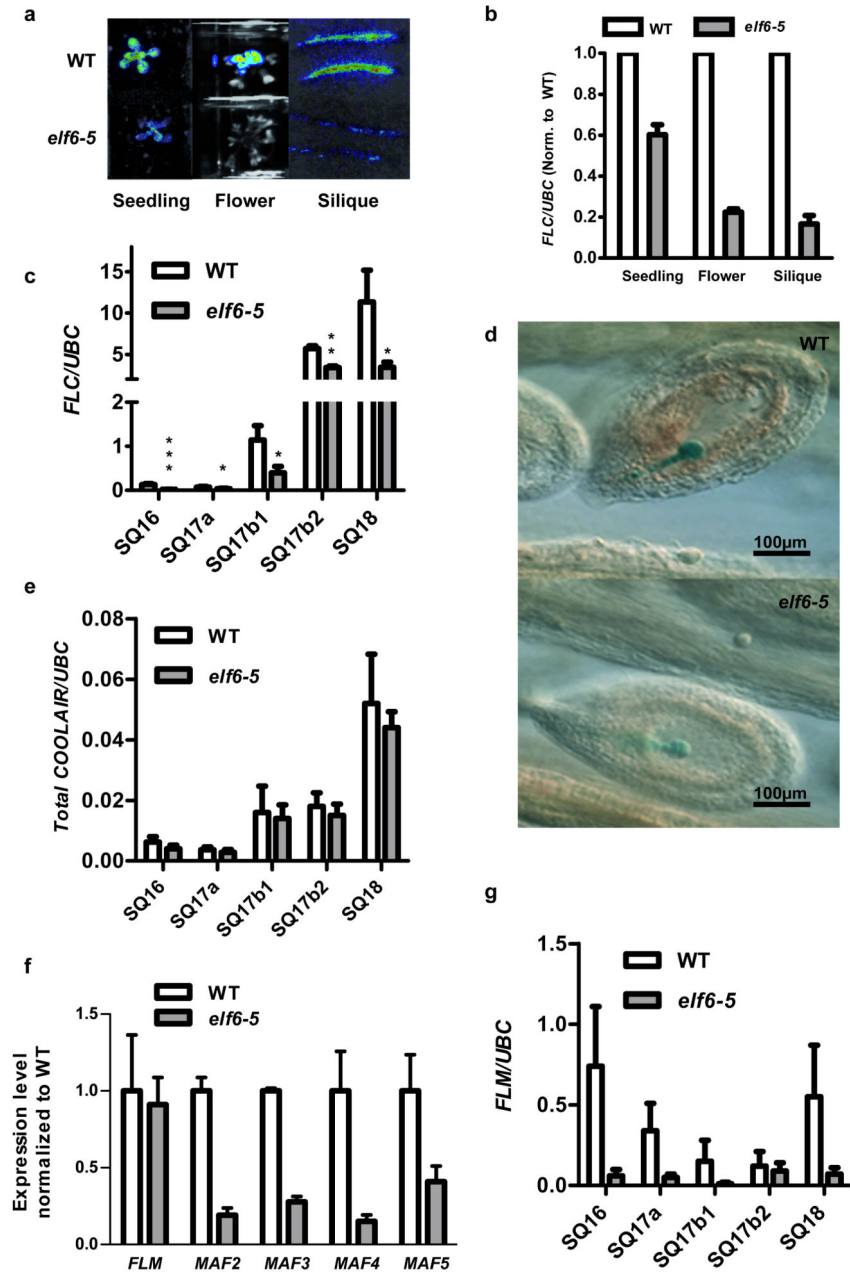


Figure 3. Characterization of the *elf6-5* resetting mutant

a, *FLC* luciferase imaging (**b**) and *FLC* Q-RT-PCR data of tissues from WT and *elf6-5* the generation following vernalization. Means \pm s.e.m., $n = 6$. **c**, Q-RT-PCR data of vernalized WT and *elf6-5* siliques¹⁸: just after fertilization with petals still attached (SQ16); small without petals (SQ17a); first (SQ17b1) and last (SQ17b2) mature green siliques; yellow siliques (SQ18). Means \pm s.e.m., $n = 4$, * $P < 0.05$, ** $P < 0.01$, *** $P < 0.001$. **d**, *FLC::GUS* expression in vernalized WT and *elf6-5* early globular embryos. **e**, Q-RT-PCR shows *COOLAIR* levels are not affected in *elf6-5* siliques. Means \pm s.e.m., $n = 5$. **f**, Q-RT-PCR showing that *MAF2-5* genes are misregulated in *elf6-5* seedlings a generation

following vernalization. Means + s.e.m., n = 3. **g**, *FLM* has reduced expression in *elf6-5* vernalized siliques. Means + s.e.m., n = 3.

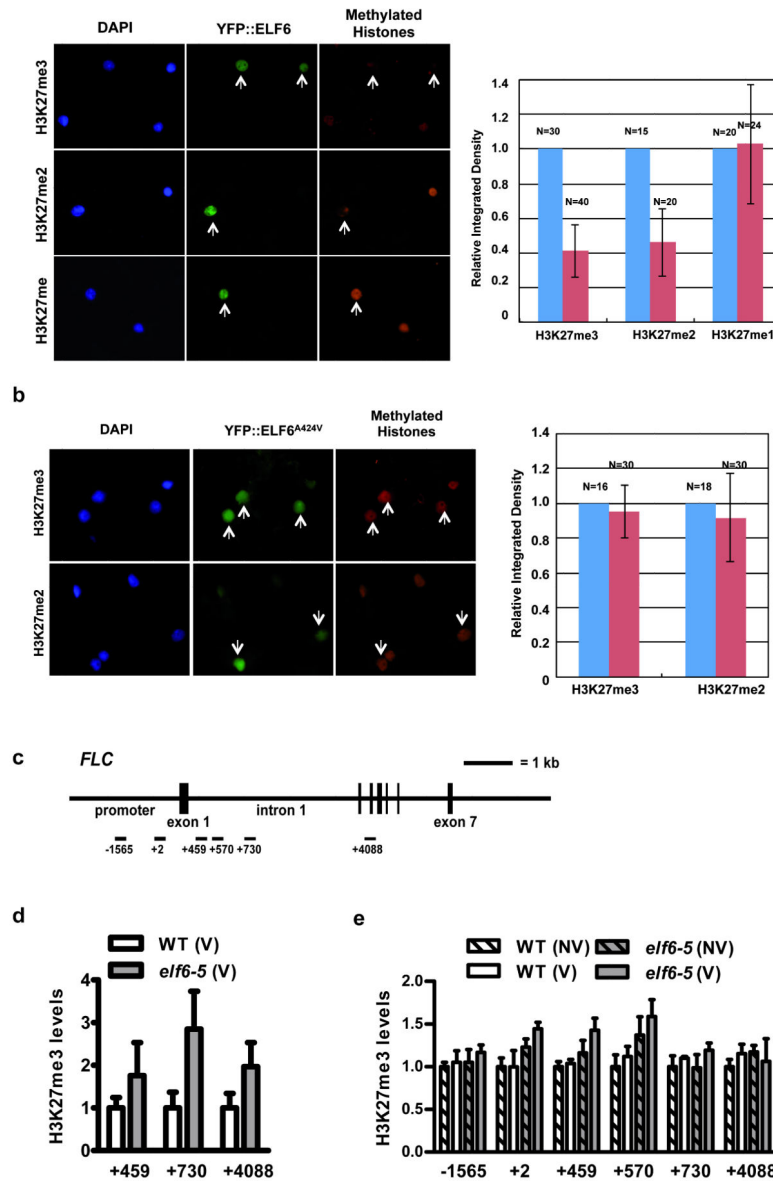


Figure 4. ELF6 shows H3K27 histone demethylase activity

a, Overexpression of a YFP::ELF6 fusion protein reduces H3K27me3, H3K27me2 but not H3K27me1. **b**, Overexpression of YFP::ELF6^{A424V} has no effect on H3K27 methylation. Histone methylation was visualized by immunostaining (red; right panels). Transfected nuclei (arrowed) were visualized by YFP signal (green; middle panels), and stained with DAPI (blue; left panels). Graphs quantify methylation levels of transfected (red) versus non-transfected (blue) nuclei. Means \pm s.d. **c**, *FLC* regions analysed in ChIP. **d**, H3K27me3 levels in *elf6-5* and WT siliques (stage SQ16-SQ17a) from vernalized plants. Means + s.e.m., $n = 3$. H3K27me3 in WT (V) plants is significantly lower than *elf6-5* (V) in *FLC* region +4088 at $*P < 0.05$. **e**, H3K27me3 levels in progeny derived from parents that had

(V) or had not (NV) been vernalized. Means + s.e.m., $n = 3$. H3K27me3 in WT (V) plants is significantly lower than *elf6-5* (V) in *FLC* region +459 at $*P < 0.05$.